Full Paper

Propellants, Explosives, Pyrotechnics

DOI: 10.1002/prep.201900389

Rapid Assembly and Preparation of Energetic Microspheres LLM-105/CL-20

Yuanping Zhang,[a] Conghua Hou,*[a] Congcong Li,[a] Xin Zhang,[a] Yingxin Tan,[a] and Jingyu Wang*[a]

Abstract: A novel composite microsphere of 2,4,6,8,10,12-hexanitrohexaazaisowurtzitane (CL-20) and 2,6-diamino-3,5-dinitropyrazine-1-oxide (LLM-105) were fabricated by spray drying technology. The morphology, structure and thermal behavior of the obtained particles were characterized via scanning electron microscopy (SEM), fourier transform infrared spectroscopy (FT-IR), powder x-ray diffraction (PXRD) and differential scanning calorimetry (DSC). SEM results demonstrated that LLM-105/CL-20 microspheres in range of 1–3 μm are relatively uniform. PXRD and FT-IR indicated that the peak patterns of the composite LLM-105/CL-20 has shifted slightly from the raw material. Thermal analysis implied that energetic microspheres LLM-105/CL-20 has lower decomposition. In addition, a possible formation mechanism for energetic microsphere was proposed. Moreover, the impact sensitivity of composite microspheres could be reduced 5 times compared to the raw CL-20. This work may introduce a novel idea towards fabricating the composite microspheres.

Keywords: LLM-105 · CL-20 · Energetic microspheres · Sensitivity

1 Introduction

Energetic materials are such compounds that contain explosive groups or contain oxidants and combustibles that can react independently and output energy, including gunpowder, explosives, and propellants, which plays a very important role in the development of national defense [1]. However, high energy and safety have always been an inherent contradiction [2]. In order to balance this conflict, several methods have been carried out including design and synthesis new structure energetic materials [3], refinement technology to improve the particle size and morphology [4], and preparing the polymer-bonded explosive (PBXs) via coating [5–6]. Among these methods, there are faced with some limitations, for instance, the improvement of sensitivity is not obvious [7]. Thus, the energetic composite with reducing sensitivity has aroused great interest. A great deal of insensitive component such as 2,4,6-Trinitrotoluene (TNT), 1,3,5-triamino-2,4,6-trinitrobenzene (TATB), 3-nitro-1,2,4-triazole-5-one (NTO), p-nitroaniline (PDA) and 2,4-dinitroaniline (DNA) are adopted to combine with high-energy explosive [8–13]. Compared with CL-20, the characteristics of the impact sensitivity (H_{50}) for CL-20@PDA and CL-20@DNA composite microspheres prepared by Yanfang Zhu et al were increased by 47 cm and 44.8 cm, respectively.

It is well-known that CL-20 [14] is currently the most powerful commercially available explosive, but its high sensitivity limits its application, so reducing its sensitivity is the focus of research work. As a typical explosive, 2,6-diamino-3,5-dinitropyrazine-1-oxide (LLM-105) [15–16] can be a promising component due to the exceptional stability at high temperatures and its resistance to accidental detonation. Therefore, the existence of a promising energetic-energetic composite between LLM-105 and CL-20 (the molecular structures of LLM-105 and CL-20 are shown in Figure 1) was reasonably expected. According to the literature in other fields [17–18], spray drying is a technology to prepare composite particles rapidly, but few reports on composite explosives have been reported. Herein, composite microspheres were fabricated by integrating LLM-105 and CL-20 particles on the basis of spray drying method. And the morphology, structure, and thermal behavior of the obtained particles were systematically characterized. We be-

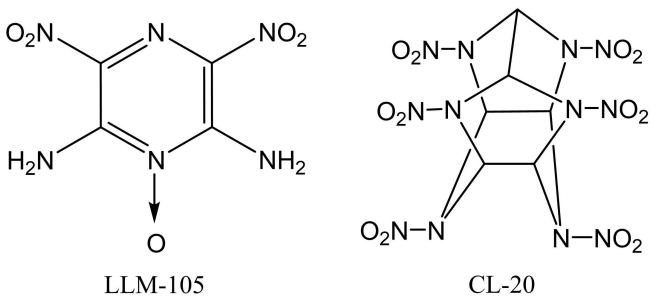

Figure 1. Molecular structure of LLM-105 and CL-20

[a] *Y. Zhang, C. Hou, C. Li, X. Zhang, Y. Tan, J. Wang*
School of Environment and Safety engineering,
North university of china,
Taiyuan Shanxi, 030051, P.R. China
**e-mail: wjywjy67@163.com*
houconghua@163.com

lieve that the facile preparation for composite microspheres endows their potential engineering amplification.

2 Experimental Section

2.1 Materials

LLM-105 was provided by Liaoning Qingyang Special Chemical Co., Ltd. CL-20 was purchased in 375 Factory of China Arms Industry Corporation. Polyvinylpyrrolidone (PVP K29) was an AR grade and purchased from Alfa Aesar. Ethyl acetate and N,N-dimethylformamide (DMF) were supplied by Sinopharm Chemical Reagent Co., Ltd.

2.2 Rapid Assembly of LLM-105/CL-20 Composite Microspheres

The fabrication of LLM-105/CL-20 composite microspheres was carried out as follows: firstly, 0.5 g CL-20 and 0.5 g LLM-105 were dissolved in the mixed solvent (the volume ratio of N,N-dimethylformamide/Ethyl acetate was 5:1). About 0.01 g polyvinylpyrrolidone (PVP) as a surfactant was added to the previous mixing system. The mixture system was sonicated and magnetically stirred for 3 hours to prepare a precursor solution. Then, the precursor solution was pumped into a small spray-drying chamber. The temperatures of inlet and outlet dry gas (N_2) were set as 120 °C and 60 °C, respectively. The spray gas flow rate was 60 L/min and the nozzle diameter is 1 mm. Finally, the products were separated from the drying gas with a cyclone separator and collected in an electrically grounded glass collection vessel. Composite particles without PVP were also prepared for comparison under the same conditions and labeled as LLM-105/CL-20 (S1), and composite particles containing PVP were labeled LLM-105/CL-20 (S2).

2.3 Characterization

The morphology of obtained samples was directly observed by the field-emission scanning electron microscope (SEM, Tescan, Czech Republic) measurements with an instrument MIRA3 LMH at an operating voltage 25 kV. The crystal phases of raw LLM-105, CL-20, and microspheres were examined by powder X-ray diffraction (PXRD, Dandong Haoyuan Corporation, Liaoning, China) with Bruker D8 Advance diffractometer at a voltage of 40 kV, and a current of 30 mA using Cu Kα radiation at $\lambda = 1.5418$ Å. Infrared spectra were collected on an IRTracer-100 Fourier transform infrared spectrometer (FTIR, Shimazu, Japan) over the range of 400–4000 cm^{-1}. Differential scanning calorimeter (DSC) test was recorded on a TA instrument from 40 to 400 °C, with a heating rate of 5, 10, 15, and 20 °C/min under nitrogen flow of 30 mL/min. The EXPLO5 software was used to estimate their detonation performance. The impact sensitivity test was performed using a home built Type 12 drop hammer apparatus according to GJB-772A-97 standard method 601.2. The samples (35 ± 1 mg) were subjected to an impact of a 2.500 ± 0.002 kg hammer and H_{50}, representing the drop height of 50% explosion probability [19].

3 Results and Discussion

3.1 Morphological Characterization

The morphology of raw LLM-105, raw CL-20, spray-dried CL-20, spray-dried LLM-105, and LLM-105/CL-20 composite microspheres obtained was observed by scanning electron microscopy (SEM) in Figure 2. We can see from Figure 2a that raw CL-20 is spindle-shaped with sharp edges and sizes, and the particle size ranging from 20–200 μm. The spray-dried CL-20 (Figure 2c) act as spheroidal morphology with an average size of 4 μm whose size and surface are smaller and smoother than that of raw CL-20. Figure 2b shows that raw LLM-105 is needle-like with obvious crystal defects, and has a partical size of about 50 μm. LLM-105 after spray drying (Figure 2d) is still needle-like, but the particle size is about 1 μm, which is significantly reduced. LLM-105/CL-20 (S1) and LLM-105/CL-20 (S2) are both composed of many

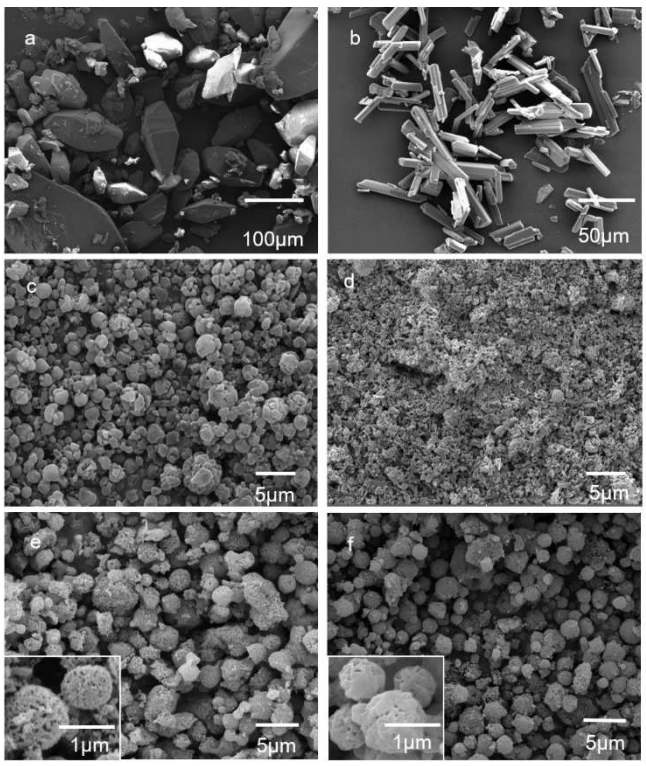

Figure 2. SEM images of raw CL-20 (a), raw LLM-105 (b), spray-dried CL-20 (c), spray-dried LLM-105 (d), LLM-105/CL-20 (S1) (e) and LLM-105/CL-20(S2) (f)

tiny particles that stick together to form a microsphere. By comparing Figure 2e and 2f, it can be found that LLM-105/CL-20 (S2) is denser than LLM-105/CL-20 (S1) because a small amount of surfactant is added to the system to obtain smoother spherical particles. It is indicated that the addition of the surfactant reduces the surface tension of the droplets, thereby facilitating the formation of spherical particles [20].

According to the spray drying theory, the formation mechanism of composite microspheres in the spray process is simply described in Figure 3. Firstly, the precursor solution is atomized into small droplets through the nozzle, and then the small droplets enter the drying chamber through the carrier gas. As the droplets have a large surface area, the solvent rapidly evaporates. Under the action of the solvent surface tension, the solute particles initially dispersed evenly in the droplets begin to self-assemble.

3.2 FTIR Analysis

In order to characterize the structure of the as-prepared composite microspheres, FTIR measurements were carried out. Infrared spectra of raw LLM-105, CL-20, and LLM-105/CL-20 composite microspheres are shown in the Figure 4. According to the infrared absorption spectrum of LLM-105/CL-20 composite microspheres in the Figure 4, it can be seen that there are peaks of CL-20 and LLM-105 in both fingerprint area (4000–1300 cm^{-1}) and characteristic area (1300-400 cm^{-1}), indicating that the composite microspheres are composed of LLM-105 and CL-20. The absorption peak of the composite microspheres shifted from that of the pure LLM-105 and CL-20, among which the absorption peak of CL-20 shifted from 3042.80 cm^{-1}, 1590.36 cm^{-1}, 1125.10 cm^{-1} to 3038.40 cm^{-1}, 1612 cm^{-1}, 1097.14 cm^{-1}; the absorption peak of LLM-105 shifted from 3225.90 cm^{-1}, 1649.84 cm^{-1}, 1247.74 cm^{-1} to 3233.43 cm^{-1}, 1640.06 cm^{-1}, 1266.56 cm^{-1}. The results indicate that there may be interactions between LLM-105 and CL-20.

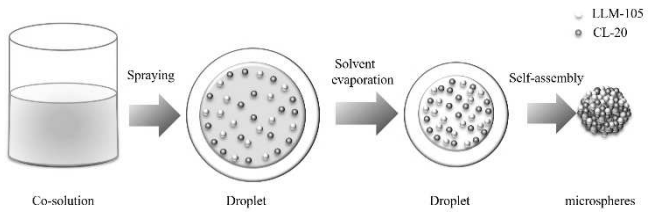

Figure 3. Schematic illustration of the formation process of LLM-105/CL-20 microsphere

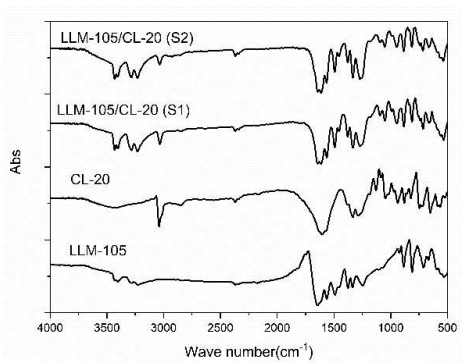

Figure 4. Infrared spectra of LLM-105, CL-20, LLM-105/CL-20 (S1) and LLM-105/CL-20 (S2)

3.3 PXRD Analysis

Powder X-ray diffraction (PXRD) is a convenient tool for analyzing the crystal structure of materials. The crystal structure of LLM-105, CL-20, and LLM-105/CL-20 composite microspheres was studied. The results are displayed in Figure 5. As can be seen from Figure 5, the main diffraction angles of raw LLM-105 localized at 11.00°, 22.25°, 24.90°, 28.50°, 33.30° corresponding to the crystal faces (1 1 0), (0 1 2), (0 4 1), (1 4 −1), (1 5 −1), which are reflected in the XRD curve of LLM-105/CL-20 composite microspheres, so the crystal form of LLM-105 before and after recrystallization has not changed. The main diffraction angles of raw CL-20 are mainly at 12.60°, 13.84°, 25.80°, and 30.44°, corresponding to the (1 1 −1), (2 0 0) (0 2 2), (2 0 −3) crystal planes, respectively, which are consistent with ε-CL-20 (PDF#00-050-2045) in the database. Compared with the ε-CL-20, the characteristic peaks of the composite microspheres were significantly shifted, added and disappeared, among which 11.94°, 13.66°, 28.30°, corresponding to the (1 1 0), (1 1 1), (1 3 2) crystal surface of β-CL-20 (PDF#00-052-2432), indicating that ε→β transition occurs in CL-20 of the composite microsphere. During the preparation of composite microspheres via spray drying, the solvent evaporates and the CL-20 crystal precipitates rapidly. In thermodynamics, the crystallization process tends to form the most stable ε crystal with the lowest free energy. However, in kinetics, the

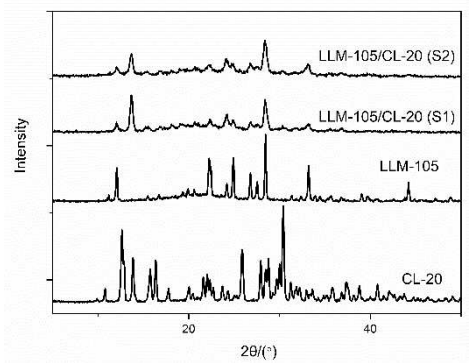

Figure 5. XRD pattern of raw LLM-105, CL-20, and LLM-105/CL-20 microsphere

formation and growth rate of metastable β crystal is much faster than that of ε crystal, which leads to the first formation of metastable β-CL-20 in solution [21]. In addition, the diffraction peaks of microspheres indicated a decrease in crystallinity, and micro/nanosizing contributed to this decrease.

3.4 Thermal Property

The thermal properties of the CL-20 and as-prepared LLM-105/CL-20 microspheres were investigated by differential scanning calorimetry (DSC). From the DSC in Figure 6, we can find that all the peaks shifted to the right as the heating rate increased.

To explore synergism reactions between components, the kinetics of the LLM-105/CL-20 microsphere with raw LLM-105 and CL-20 were further studied and compared. The thermal decomposition kinetic parameters were calculated by the Kissinger method and the Arrhenius equation commonly used in thermodynamic analysis methods [22]. Furthermore, the thermal stability of explosive can be counted by Equations (2) and (3) [7].

$$\ln\frac{\beta_i}{T_{pi}^2}=\ln\frac{AR}{E_a}-\frac{E_a}{RT_{pi}} \quad (1)$$

$$T_p=T_{p0}+b\beta_i+c\beta_i^2+d\beta_i^3 \quad (2)$$

$$T_b=\frac{E_a-\sqrt{E_a^2-4RE_aT_{p0}}}{2R} \quad (3)$$

Where β_i is the heating rate in °C/min; T_p is the peak temperature in the DSC trace at β_i in K; R is the universal gas constant (8.318 J·K^{-1}·mol^{-1}); A is the pre-exponential factor in s^{-1}; E_a is the apparent activation energy in kJ·mol^{-1}; k is the rate constant in s^{-1}; T_{p0} is the peak temperature when β_i is zero in K; b, c, and d is constant; T_b is the critical explosion temperature in °C.

Based on the peak temperature of the high-temperature decomposition of samples at 5, 10, 15, and 20 °C/min, the calculated kinetic parameters of the sample during the thermal decomposition process are listed in Table 1. It can be seen from Table 1 that the activation energy of the two thermal decomposition stages of the composite microspheres is lower than that of the raw materials, indicating that the thermal stability of the composite is lower and the heat release is more concentrated. Since the composite microspheres are assembled by nano-CL-20 and LLM-105, the specific surface area and surface atom number of the crystal grains increase remarkably with the decrease of the crystallite size, which may cause strong molecular vibration and polymer of surface molecules energy. In addition, the nanoparticles are in full contact, the interaction is enhanced, and the reaction is fully reacted during the heating process. The decomposition of CL-20 particles accelerates the decomposition of LLM-105, leading to thermal decomposition and energy concentration. This phenomenon is similar to in the literature [13].

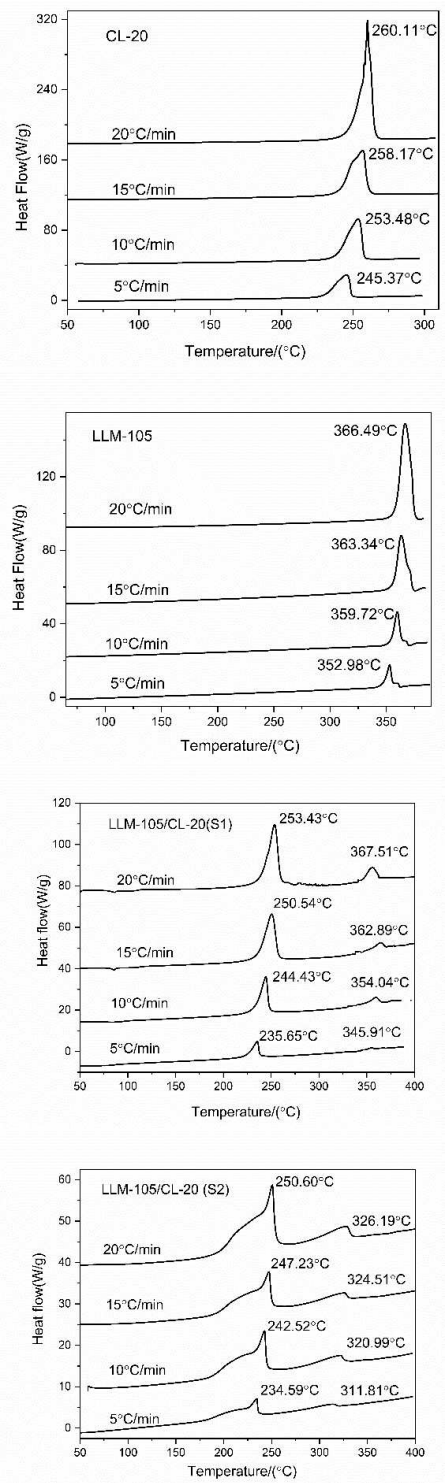

Figure 6. DSC curves of CL-20, LLM-105, LLM-105/CL-20 (S1) and LLM-105/CL-20 (S2)

Table 1. The calculated kinetic parameters of the CL-20, LLM-105 and LLM-105/CL-20 microsphere.

Sample	E_a(kJ/mol)	lgA (min^{-1})	T_{p0}(°C)	T_b(°C)
CL-20	200.91	19.88	233.17	235.46
LLM-105	332.07	24.41	340.37	343.81
LLM-105/	161.38	16.14	224.75	227.41
CL-20(S1)	194.61	15.93	343.45	348.64
LLM-105/	182.78	18.43	221.56	223.84
CL-20 (S2)	259.32	22.79	293.15	295.96

3.5 Detonation Performance

The theoretical detonation performance of LLM-105, CL-20, and LLM-105/CL-20 calculated by EXPLO5 program are shown in the Table 2. The detonation velocity and pressure of LLM-105/CL-20 composites are 9236.99 m/s and 38.84 GPa, respectively, which are equivalent to that of the current military standard explosive HMX (9124 m/s) [23].

3.6 Impact Sensitivity

The safety of explosives is the basis for their application. According to the GJB 772 A-1997 method 603.1, the impact sensitivity of the raw materials LLM-105, CL-20, LLM-105/CL-20 (S1), and LLM-105/CL-20 (S2) was tested, and the results are shown in the Table 3. It can be found that the characteristics of the LLM-105/CL-20 (S1) and LLM-105/CL-20 (S2) were 73.4 and 79.2 higher than those of the raw CL-20, respectively, so the impact sensitivity was significantly reduced. The reason for the analysis is that the prepared composite microspheres have a spheroidal structure and contain the insensitive component LLM-105. When exposed to external stimuli, the propagation is hindered, the probability of hot spot formation is effectively reduced, the explosion probability is reduced. In particular, the characteristic drop height of LLM-105/CL-20 (S1) is higher than that of LLM-105/CL-20 (S2). This is because the existence of PVP makes the surface of composite microsphere smooth and difficult to form hot spots, so the impact sensitivity is lower.

Table 2. Detonation performance of LLM-105, CL-20 and LLM-105/CL-20 composites.

Samples	Density/ $g\,cm^{-3}$	Velocity/ ($m\,s^{-1}$)	Pressure (GPa)	Temperature/K
CL-20	2.038	9762.05	44.66	4097.97
LLM-105	1.913	8751.67	33.19	3265.86
LLM-105/CL-20	1.974	9236.99	38.84	3672.52

Table 3. Impact sensitivity of samples.

Samples	H_{50}(cm)
CL-20	14.60
LLM-105	125
LLM-105/CL-20 (S1)	88
LLM-105/CL-20 (S2)	93.8

4 Conclusion

In summary, a novel LLM-105/CL-20 composite microspheres were fabricated by spray drying. The SEM images directly showed the morphologies of as-obtained samples are composite microsphere in range of 1–3 μm. And the crystal structure was characterized by FTIR and XRD. From the results of thermal analysis, LLM-105/CL-20 energetic microspheres has lower decomposition. Interestingly, the LLM-105/CL-20 energetic microspheres maintain the excellent energetic properties with the detonation pressure and detonation velocity as 9236.99 m/s and 38.84 GPa, which is equivalent to that of the HMX. Meanwhile, the mechanical sensitivities of LLM-105/CL-20 composite microsphere were reduced 5 times significantly compared to that of raw CL-20. It can be concluded that the LLM-105/CL-20 composite microsphere can balance the contradiction between high energy and insensitive. This work may introduce a novel idea towards fabricating the composite microspheres and expand the scope of application of explosives.

Acknowledgments

This research work was financially supported Graduate Education Innovation Project in Shanxi Province (2018BY089).

References

[1] S. F. Son, R. A. A. Yetter, V. Yang, Introduction: nanoscale composite energetic materials, *J. Propul. Power.* **2007**, *23*, 643–644.
[2] A. K. Sikder, N. Sikder, A Review of Advanced High Performance, Insensitive and Thermally Stable Energetic Materials Emerging for Military and Space Applications, *J. Hazard. Mater.* **2004**,*112*, 1–15.
[3] Y. Xu, Q. Wang, C. Shen, Q. Lin, P. Wang, M. Lu, A series of energetic metal pentazolate hydrates, *Nature* **2017**, *549*, 78–81.
[4] Y. Zhang, C. Hou, X. Jia, J. Wang, Y. Tan, Fabrication of Nanoparticle-Stacked 1,1-Diamino-2,2-Dinitroethylene (FOX-7) Microspheres with Increased Thermal Stability, *J. Nanomater.* **2019**.
[5] A. Elbeih, S. Zeman, M. Jungová, P. Vávra, Attractive nitramines and related PBXs, *Propellants Explos. Pyrotech.* **2013**, *38*, 379–385.
[6] X. Jia, J. Wang, C. Hou, Y. Tan, Y. Zhang, Effective Insensitiveness of Melamine Urea-Formaldehyde Resin via Interfacial Polymerization on Nitramine Explosives, *Nanoscale Res. Lett.* **2018**, *13*, 402.
[7] C. Hou, X. Jia, J. Wang, Y. Tan, Y. Zhang, C. Li, Efficient preparation and performance characterization of the HMX/F2602 microspheres by one-step granulation process, *J. Nanomater.* **2017**.

[8] C. An, J. Wang, W. Xu, F. Li, Preparation and Properties of HMX Coated with a Composite of TNT/Energetic Material. *Propellants Explos. Pyrotech.* **2010**, *35*, 365–372.
[9] C. Hou, Y. Zhang, Y. Chen, X. Jia, Fabrication of Ultra-fine TATB/HMX Cocrystal Using a Compound Solvent, *Propellants Explos. Pyrotech.* **2018**, *43*, 916–922.
[10] G. Yang, F. Nie, Preparation and Characterization of Core/shell Structure of HMX/NTO Composite Particles. *Sci. Technol. Energ. Mater.* **2006**, *67*, 77–81.
[11] K. J. Kim, H. S. Kim, Agglomeration of NTO on the Surface of HMX Particles in Water-NMP Solvent. *Cryst. Res. Technol.* **2008**, *43*, 87–92.
[12] Y. Zhu, Y. Lu, B. Gao, D. Wang, G. Yang, C. Guo, Ultrasonic-assisted emulsion synthesis of well-distributed spherical composite CL-20@PNA with enhanced high sensitivity, *Mater. Lett.* **2017**, *205*, 94–97.
[13] Y. Zhu, J. Luo, Y. Lu, H. Li, B. Gao, D. Wang, Emulsion synthesis of CL-20/DNA composite with excellent superfine spherical improved sensitivity performance via a combined ultrasonic–microwave irradiation approach, *J. Mater. Sci.* **2018**, *53*,14231–14240.
[14] J. H. Urbelis, V. G. Young, J. A. Swift, Using solvent effects to guide the design of a CL-20 cocrystal. *CrystEngComm* **2015**, *17*, 1564–1568.
[15] C. M. Tarver, P. A. Urtiew, T. D. Tran, Sensitivity of 2,6-Diamino-3,5-Dinitropyrazine-1-Oxide. *J. Energ. Mater.* **2005**, *23*, 183–203.
[16] P. Deng, Y. Liu, P. Luo, J. Wang, Y. Liu, D. Wang, Y. He, Two-steps synthesis of sandwich-like graphene oxide/LLM-105 nano energetic composites using functionalized graphene, *Mater. Lett.* **2017**, *194*, 156–159.
[17] A. Gharsallaoui, G. Roudaut, O. Chambin, A. Voilley, R. Saurel, Applications of spray-drying in microencapsulation of food ingredients: An overview. *Food Res. Int.*, **2007**, *40*, 1107–1121.
[18] R. Vehring, Pharmaceutical particle engineering via spray drying. *Pharm. Res.*, **2008**, *25*, 999–1022.
[19] National Defense Science and Technology Committee. GJB 772A-1997: National Military Standard of China. Beijing: Military standard press of the national defense science and technology commission, **1997**.
[20] X. Zhou, Q. Zhang, R. Xu, D. Chen, S. Hao, A Novel Spherulitic Self-Assembly Strategy for Organic Explosives: Modifying the Hydrogen Bonds by Polymeric Additives in Emulsion Crystallization, *Cryst. Growth Des.* **2018**, *18*, 2417–2423.
[21] M. Ghosh, V. Venkatesan, S. Mandave, Probing crystal growth of ε-and α-CL-20 polymorphs via metastable phase transition using microscopy and vibrational spectroscopy, *Cryst. Growth Des.* **2014**, *14*, 5053–5063.
[22] HE. Kissinger, Reaction kinetics in differential thermal analysis. *Anal. Chem.* **1957**, *29*, 1702–1706.
[23] B. Y. Ye, C. W. An, J. Y. Wang, X. H. Geng, Formation and properties of HMX-based microspheres via spray drying, *RSC Adv.* **2017**, *7*, 35411–35416.

Manuscript received: November 20, 2019
Revised manuscript received: March 9, 2020
Version of record online: May 26, 2020

